Saudi Pharmaceutical Journal 30 (2022) 485–493

Contents lists available at ScienceDirect

Saudi Pharmaceutical Journal

journal homepage: www.sciencedirect.com

Original article

Methoxybenzamide derivative of nimesulide from anti-fever to anti-cancer: Chemical characterization and cytotoxicity

Laila A. Jaragh-Alhadad *, Mayada S. Ali

Chemistry Department, Kuwait University, P. O. Box 5969, Safat 13060, Kuwait

ARTICLE INFO

Article history:
Received 1 December 2021
Accepted 5 March 2022
Available online 10 March 2022

Keywords:
Nimesulide
HSP27
Crystal structure
H292
SKOV3
SKBR3
Anti-cancer agent

ABSTRACT

The repurposing strategy of converting nimesulide from an anti-fever drug to an anti-cancer agent by modifying its main structure targeting HSP27 is gaining great attention these days. The goal of this study focuses on synthesizing a new nimesulide derivative with new ligands that have biological anti-cancer activities in different cancer models using the in-vitro assay. Nimesulide derivative L1 was synthesized, characterized by 1H NMR, 13C NMR, FTIR, melting point, mass spectra, and TGA analysis. A single crystal was diffracted and showed colorless block group P-1. The results revealed that L1 demonstrates potent anti-cancer activity with lung (H292), ovarian (SKOV3), and breast (SKBR3) cancer cell lines in-vitro models with IC_{50} values below 8.8 μM.

1. Introduction

Cancer accounts for a significant portion of deaths around the world (Zaorsky et al., 2017; Chu et al., 2018; Mahase, 2019; Zhang et al., 2020). In 2016, the number of new lung cancer cases diagnosed was increased to 14% and remained the highest mortality rate accounting for about one in four cancer deaths (Han-Shui et al., 2011; Zakaria et al., 2017). Moreover, ovarian cancer is the fifth leading cause of cancer death in women and the most lethal gynecologic malignancy (Aletti et al., 2007; Jemal et al., 2010). Most patients present with late ovarian cancer stages their survival rate is 45% within five years (Aletti et al., 2007). In addition, breast cancer is common cancer among females worldwide with an incidence rate of over 1.6 million cases per year, but patients' survival rates reach 99% if the tumor is diagnosed in the early stages (Torre et al., 2012; Jin and Mu, 2015). Therefore, it is urgently required to develop new drugs for cancer therapy (Jorg et al., 2016; Zhang et al., 2020).

Several reviews summarized the evidence that non-steroidal anti-inflammatory drugs (NSAIDs) are characterized by anticancer properties (Taketo, 1998; Janne et al., 2000). Inflammation is associated with cancer and plays an important role in tumor development and progression (Aggarwal et al., 2006; Zappavigna et al., 2020). NSAID drugs are COX-2 inhibitors (Piazza et al., 2010) and have proved experimentally to stimulate apoptosis (Zappavigna et al., 2020) and inhibit angiogenesis (Thun et al., 2002).

In addition, studies proved that the nimesulide drug is one of the NSAID drugs (Ward and Broagden, 1988; Giuliano & Warner, 1999) and is characterized for its anti-proliferation property (Banti et al., 2016; Catarro et al., 2019; Jaragh-Alhadad et al., 2018 & 2022). Furthermore, Banti et al. synthesized and characterized nimesulide derivatives silver metallodrugs. The results showed in-vitro cytotoxicity with the MCF7 breast cancer cell line by altering the apoptotic pathway mitochondrial damage (Banti et al., 2016). A further research study showed 5-aminosalicylic acid in combination with nimesulide inhibited the proliferation of colon carcinoma cells in-vitro (Hai-Ming et al., 2007). Jian et al. studied hyaluronic acid conjugated to nimesulide as an anticancer drug and the results showed cell death in CD44 overexpressing HT-29 cells in-vitro and inhibited tumor growth in-vivo (Jian et al., 2016). Kankanala et al., synthesized nimesulide-based novel glycol amide esters, and the compounds were cytotoxic against HCT-15 human colon cancer cell line (Kankanala et al., 2013). In 2022, nimesulide derivatives were synthesized to target the function of HSP27 in both SKOV3 and SKBR3 cell lines and the results showed

* Corresponding author.
E-mail address: laila.alhadad@ku.edu.kw (L.A. Jaragh-Alhadad).

Peer review under responsibility of King Saud University.

Production and hosting by Elsevier

https://doi.org/10.1016/j.jsps.2022.03.004

potent promising agents for future chemotherapy (Jaragh-Alhadad et al., 2022).

Heat shock protein (HSP27) protein acts as an anti-apoptotic protein (Zhengyong et al., 2021) when facing stressful conditions such as chemotherapy drugs (Zhang et al., 2007; Vidyasagar, 2012). When a patient is receiving chemotherapy drugs, HSP27 phosphorylation increases tubulin polymerization, proliferation and stops the apoptotic pathways (Charette and Landry 2000; Xi et al., 2015). HSP27 promotes cancer cells division and metastasis (Han-Shui et al., 2001; Calderwood, 2006; Casado et al., 2007) and is overexpressed in many types of human cancer: including gastric (Hua et al., 2017), liver (Jorg et al, 2017), prostate (Rocchi et al., 2005), rectal (Haiping et al., 2017), lung (Baowei et al., 2017), ovarian (Jaragh-Alhadad et al., 2018 & 2022; Jaragh-Alhadad and Samir, 2021) and breast cancer (Calderwood et al., 2006; Vidyasagar et al., 2012**)**. In addition, to its pronounced treatments' resistance in breast (Vidyasagar et al., 2012), colon, leukemia (Ciocca and Calderwood, 2005**),** and ovarian cancers (Jaragh-Alhadad et al., 2018 & 2022; Jaragh-Alhadad and Samir, 2021**)**. In Sum, HSP27 is an attractive molecular target for anti-cancer drug design.

Therefore, the development of old drugs for new and faster therapeutic purposes is urgently required (Zhang et al., 2020)**.** This strategy provides further benefits because the drug is already administered to patients and no need for further clinical trials (Mahase, 2019; Jaragh-Alhadad et al., 2021)**.** Therefore, the goal of this study is to use nimesulide as a starting material for the synthesis of agent L1 with new ligands added to its skeleton and spectroscopically characterized (Jaragh-Alhadad and Samir, 2021; Jaragh-Alhadad et al., 2022). Finally, the cytotoxic activities of agent L1 were treated with H292, SKOV3, and SKBR3 cancer models.

2. Materials and methods

2.1. Chemicals

All chemicals and solvents such as 2-Amino-5-nitrophenol, acetyl chloride, dimethylformamide (DMF), potassium carbonate (K_2CO_3), sodium hydride (NaH), ferric chloride ($FeCl_3$), and dioxane products purchased from Sigma-Aldrich, Germany, and E. Merk, were used as received directly without further preparation. The elemental (C, H, and N) content of agent N-(4-acetamido-3-((2,5 dimethyl benzyl) oxy) phenyl)-4- methoxybenzamide L1, was determined at the Microanalytical Unit (Varian Micro V1.5.8, CHNS Mode, 15073036) at Kuwait University. Fourier transform infrared (FTIR) spectrum was with potassium bromide (KBr) discs on an FTIR-6300 type a (400–4000 cm^{-1}). Nuclear magnetic resonance (NMR) spectra of the agent were recorded in dimethyl sulfoxide (DMSO) d6, on a Bruker WP 200 SY spectrometer (400 MHz) at room temperature (25 °C) using tetramethylsilane (TMS) as external standard. Thermal gravimetric analysis (TGA) was measured at (10–850 °C) on a Shimadzu TGA-60; the nitrogen flow and heating rates were 50 ml/min and 10 °C respectively. The X-ray single-crystal diffraction data were collected using filtered Mo Ka-radiation on a Rigaku R-Axis Rapid diffractor meter. Confirmation of agent L1 structure was by the direct methods and expanded using Fourier techniques at Kuwait University.

Lung (H292), ovarian (SKOV3), breast (SKBR3) cancer cell lines, and the healthy kidney (HEK293) cells are from ATCC (Rockville, MD). Cell Culture media and other supplements, such as fetal bovine serum (FBS), phosphate buffer saline (PBS), trypsin, L-glutathione, penicillin-streptomycin, and 3-(4,5-dimethylthia zol-2-yl)-2,5-diphenyl-2H- tetrazolium bromide (MTT assay), were

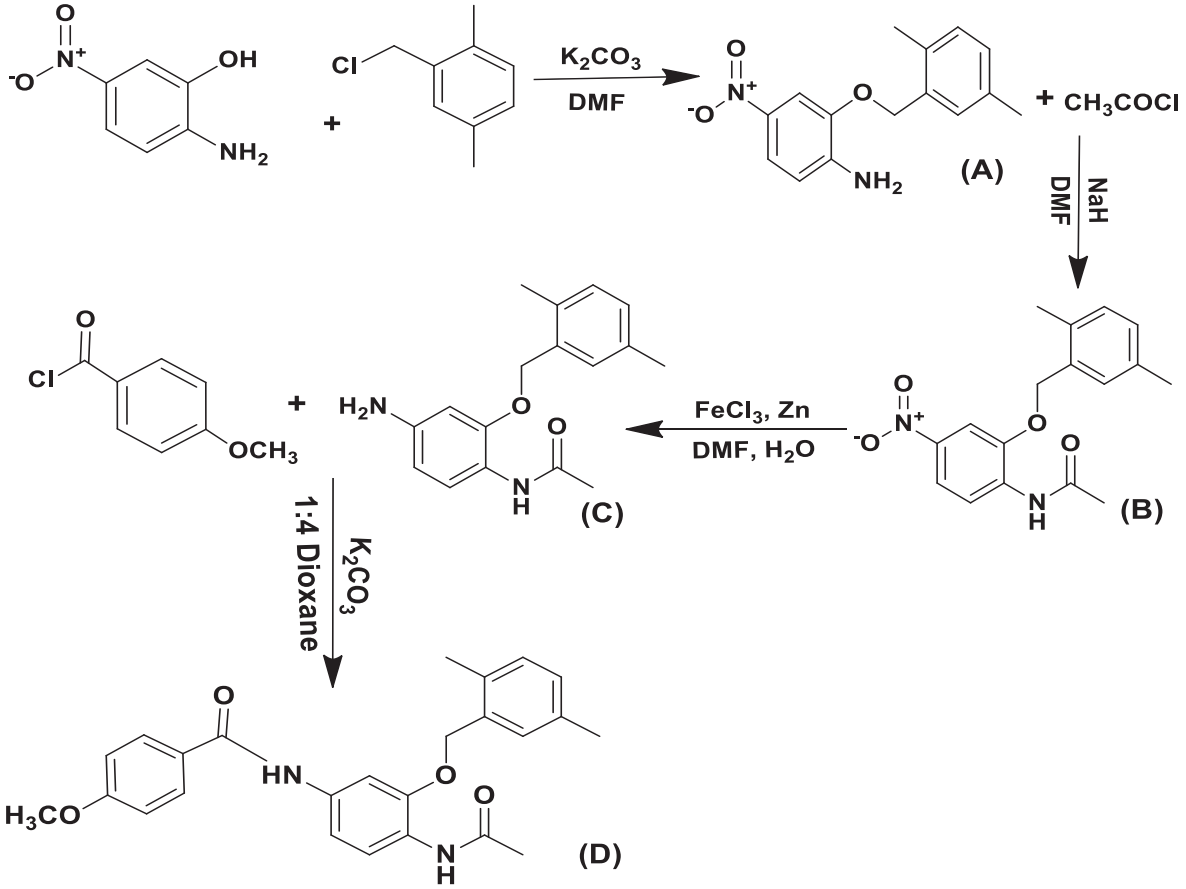

Scheme 1. Synthesis steps of agent L1, N-(4-acetamido-3-((2,5-dimethylbenzyl) oxy) phenyl)-4- methoxybenzamide.

obtained from Sigma-Aldrich (Milwaukee, WI) and ready for direct use without the need for any preparation. Biological parameters were examined at Kuwait University.

2.2. Single-crystal data collection and structure refinement

In this study, the crystal structure of agent L1 was grown by dissolving 15.0 mg in one ml of hot ethanol. The solution was covered with parafilm with holes to allow slow evaporation then a suitable crystal was ready for diffraction within a week. A single crystal data analysis was made by a Bruker SHELXTL Software Package using a narrow-frame algorithm. The absorption effects are determined by the multi-scan method (SADABS). The ratio of minimum to the maximum apparent transmission was 0.571. The calculated minimum and maximum transmission coefficients (based on crystal size) are 0.1970 and 0.5840.

2.3. Synthesis of N-(4-acetamido-3-((2,5-dimethylbenzyl)oxy) phenyl)-4- methoxybenzamide: Agent L1

Starting with 2-Amino-5-nitrophenol (0.154 g; one mmol) and 2-(chloromethyl)-1,4-dimethyl benzene (0.154 g; one mmol) in the presence of K_2CO_3 (0.138 g; one mmol) and DMF, left overnight to obtain compound (A). In the next step, both acetyl chloride (0.078 g; one mmol) and NaH (0.12 g; five mmol) were added in dry DMF at room temperature to obtain compound (B) within an hour. Then, $FeCl_3$ is added (0.648 g; four mmol) to DMF and water, stirring for 15 min. Next, the addition of zinc powder (6.5 g; ten mmol) to reduce the nitro group to an amine group and obtain the compound (C). Then, 4-methoxybenzoyl chloride; was added to compound (C), K_2CO_3 and 1:4 dioxane to obtain the final compound (D), which is agent L1 as described in Scheme 1. Synthesis steps carried out at room temperature, agent L1 was precipitated out, filtered, grown, and diffracted as a single crystal.

2.4. Cytotoxicity assay

Cancer cells were maintained in Roswell Park Memorial Institute (RPMI1640) medium supplemented with 10% FBS (inactivated for 30 min in a water bath before use) and 1% penicillin-streptomycin and 1% L-glutathione. Cell cultures were grown in a 5% CO_2 incubator (Bridgeport N.J.). In-vitro evaluation cytotoxicity assay was applied using 3-(4,5-dimethylthiazol-2-yl)-2,5-diphe nyl-2H- tetrazolium bromide (MTT assay) in six replicates. First, cells were grown in RPMI1640 medium in 96-well plates for 24 hr. Second, cells were exposed to various concentrations of the agents dissolved in DMSO (final concentration $\leq$ 0.1%) in media for 48 hr. The medium was removed, replaced by 200 µL of 0.5 mg/ml of MTT in new media followed by incubation for two hrs. Supernatants; were removed, and the dye was solubilized in

Table 1
Structural parameters of agent L1.

Parameter	Agent L1
Formula weight	418.48
Chemical formula	$C_{25}H_{26}N_2O_4$
Temperature	296(2) K
Wavelength	Cu Kα (λ = 1.54178 Å)
Crystal system	triclinic
Crystal size	0.060 × 0.080 × 0.160 mm
Crystal habit	colorless Block
Space group	P −1
Unit cell dimensions	
a (Å)	10.1755(8)
b (Å)	10.6614(9)
c (Å)	11.8916(11)
α (°)	71.702(4)
β (°)	76.728(4)
γ (°)	65.653(3)
Density (g/cm^3)	1.254
F(000)	444
θ the range for data collection (°)	3.94 to 66.44
Volume (Å^3)	1108.40(17)
Z	2
Absorption coefficient (mm^{-1})	0.690
Measured reflections	13,237
Independent reflections	3787 [R(int) = 0.0478]
Observed reflections	1380
Refinement method	Full-matrix least-squares on F^2
Final R indices (observed data)	R1 = 0.0682, wR2 = 0.2281
R indices (all data)	R1 = 0.0800, wR2 = 0.2348
Goodness-of-fit on F2	1.171
Largest diff. peak and hole (eÅ^{-3})	0.239 and −0.269

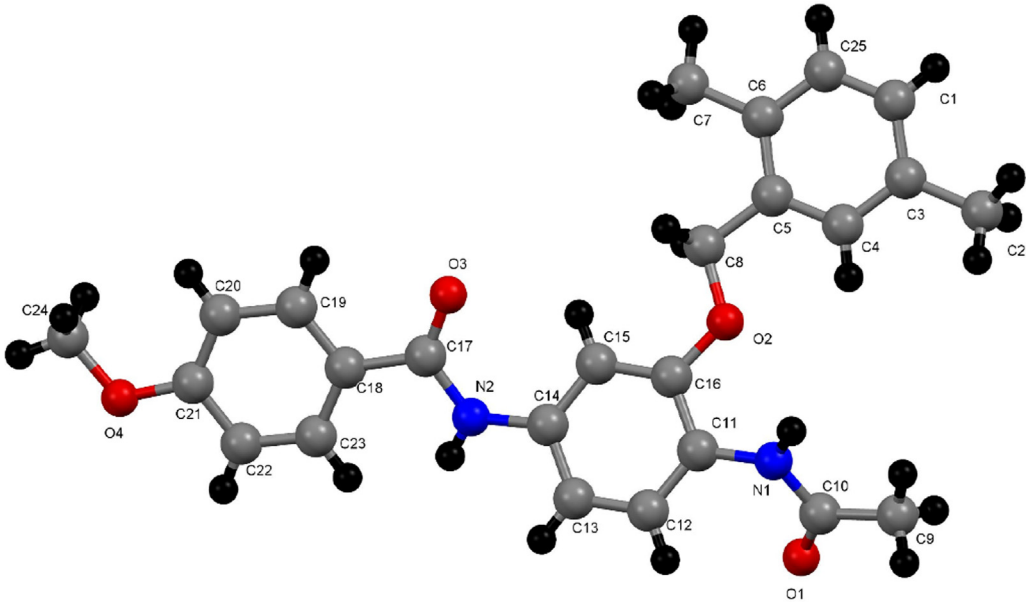

Fig. 1. Crystal structure of nimesulide derivative, agent L1.

Table 2
Bond lengths and angles for agent L1.

Agent (L1)			
Bond lengths (Å)		Bond angles (Å)	
O1-C10	1.223(5)	C8-O2-C16	118.3(3)
O3-C17	1.228(4)	C21-O4-C24	118.0(3)
N1-C11	1.420(4)	C11-N1-C10	125.0(3)
N2-C14	1.412(4)	C14-N2-C17	128.6(3)
O2-C16	1.362(4)	N1-C10-O1	122.9(4)
O4-C21	1.367(4)	N2-C17-O3	123.0(3)
O2-C8	1.421(4)	C10-N1-H	117.5
O4-C24	1.421(5)	C17-N2-H	115.7
N1-H	0.86	O4-C24-H	109.5
N2-H	0.86	O1-C10-C9	122.0(3)

200 μL/well DMSO. The plate reader; was used to determine the absorbance at 570 nm.

2.5. Statistical analysis

The statistical and graphical information was determined using Graph Pad Prism software (Graph Pad Software Incorporated) and Microsoft Excel (Microsoft Corporation). IC_{50} values were determined using nonlinear regression analysis.

3. Results

In this study, agent L1 is found to be soluble in solvents such as methanol, ethanol, DMSO, $CHCl_3$, acetone, and water (Ferreira

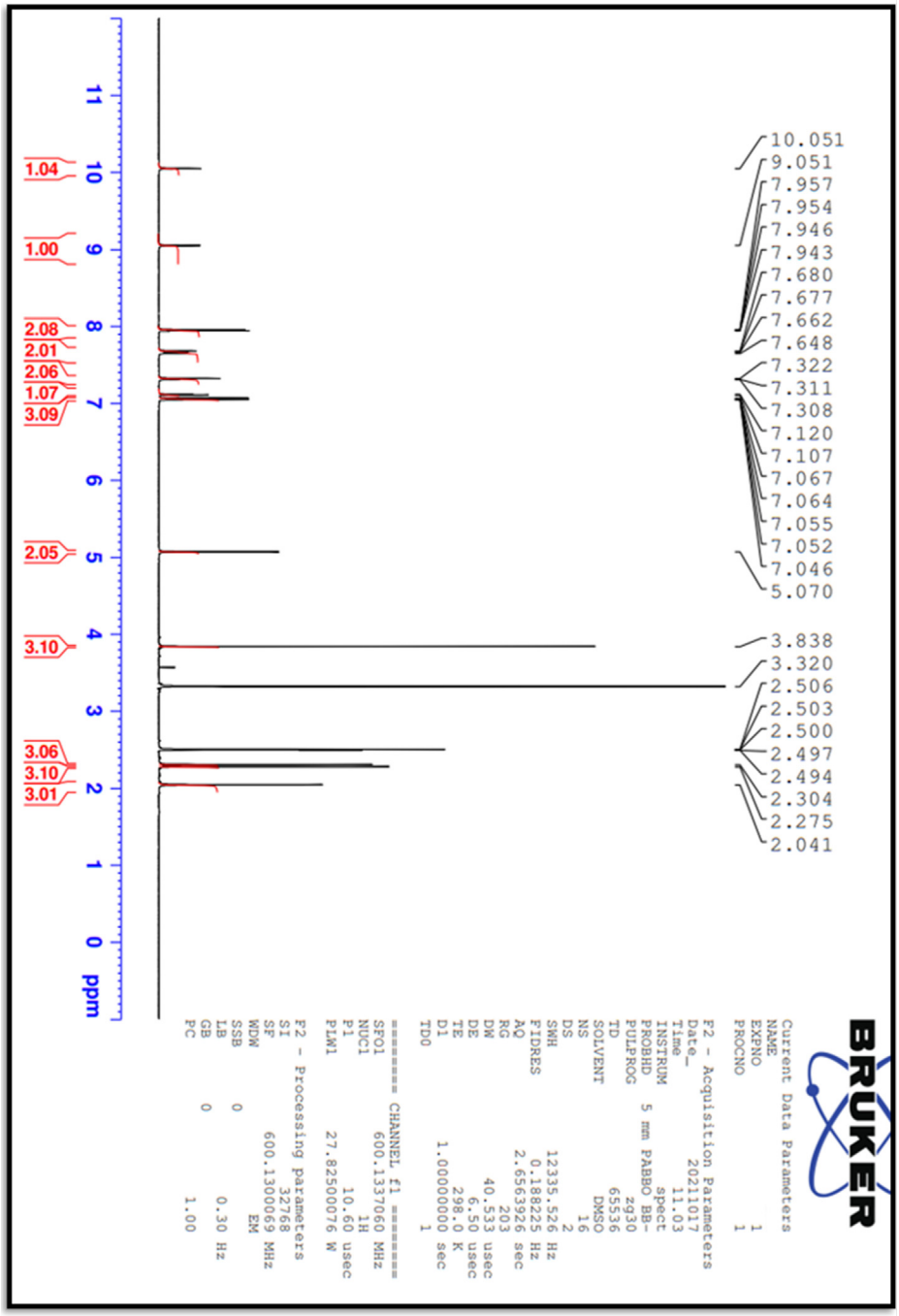

Fig. 2. 1H NMR spectrum of agent L1.

et al., 2021). Agent L1 purity was tested by elemental analysis, FTIR, 1H NMR, and 13C NMR. Element's analysis data are consistent with the calculated results from the empirical formula of the agent. This indicates that agent L1 is purely more than 95%. X-ray crystallography technique confirmed agent L1 structure. In addition, the agent L1 melting point was more than 350 °C which indicates its stability. Furthermore, TGA analysis data showed a stable agent until the temperature reaches 550 °C, and then the agent starts to break down.

X-ray crystallographic data collection and structural refinement of agent L1 is viewed in (Fig. 1), the results were summarized in (Tables 1 & 2) and showed a colorless block with the formula $C_{25}H_{26}N_2O_4$ and a molecular weight of 418.48, which belongs to the triclinic system with the P-1 space group. Table 2 data demonstrates that C(10)—O(1) and C(17)—O(3) bond length of 1.223(5) and 1.228(4)Å respectively, within the values of C=O double bond. The C(11)—N(1) and C(14)—N(2) bond lengths are equal. The C8-O2 bond length of 1.421 Å is in the range of a single C—O bond.

The 1H NMR spectrum (Fig. 2) exhibited two broad bands at d 10.051 and 9.051 ppm assigned to NH protons. The protons of aromatic CH appear at 7.957–7.046 (m, 10*H*) ppm and signal at 5.07 ppm (s, 2H) for CH_2 protons, whereas for CH_3O protons appear at 3.838 ppm and 2.506–2.041 (m, 9H) ppm for the CH_3 protons. 13C NMR data (Fig. 3) showed different peaks at 168.21, 149.89,

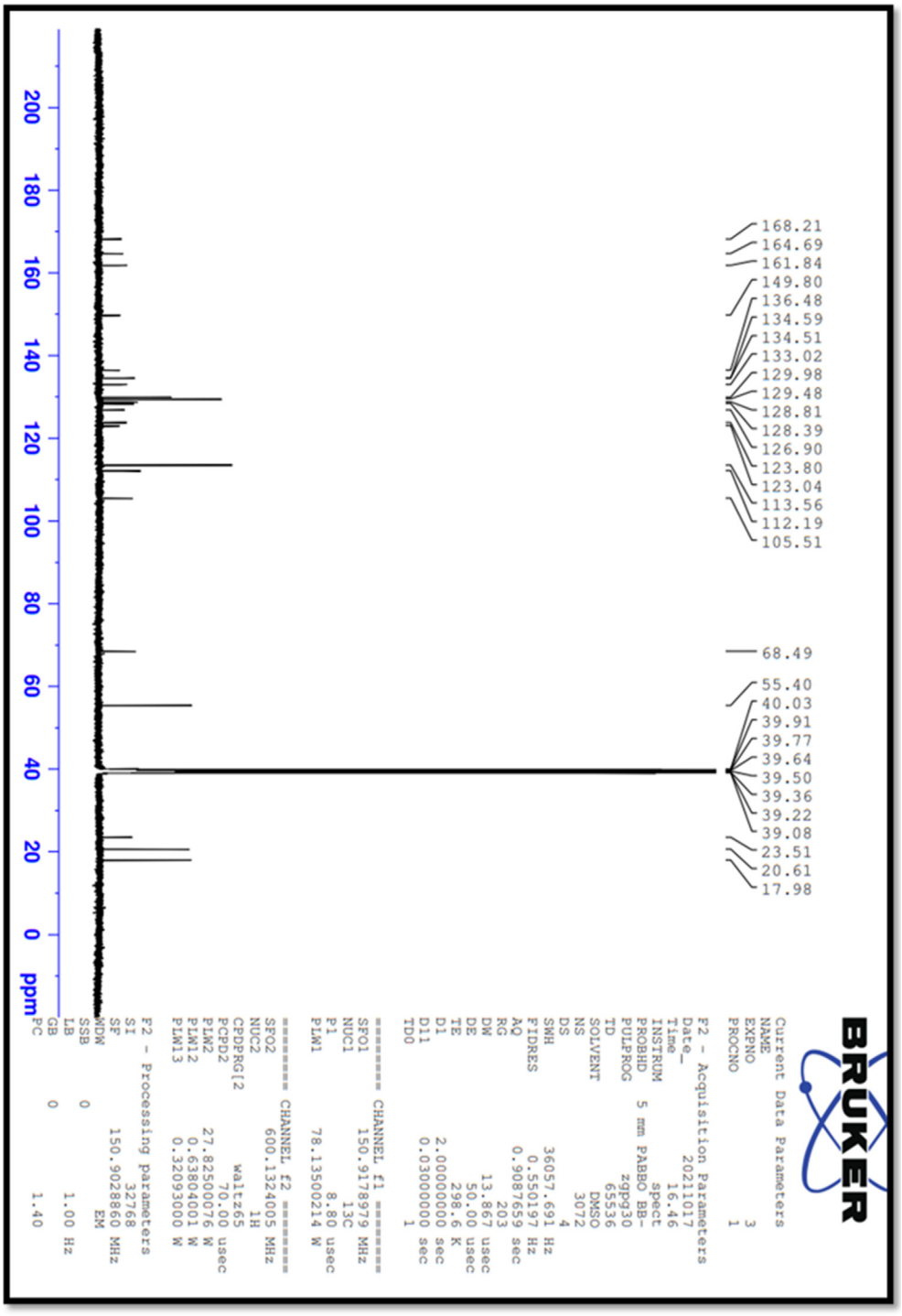

Fig. 3. 13C NMR spectrum of agent L1.

136.48, 105.51, and 68.49 ppm due to C═O, C—O, C—N, C═C, and CH_3, respectively. NMR analysis of agent L1 in DMSOd_6 summarized in (Table 3).

The major FTIR bands of agent L1 are listed in (Table 3), the spectrum showed two broad bands at (3328–3276) cm^{-1} attributed to ν(NH) and other bands at (1660–1639), 1607, 1256 cm^{-1} attributed to ν(C═O), ν(C—N), ν(C—O) respectively (Fig. 4). The appearance of (CH_3O) bands at (1048–1031 cm^{-1}) and at (829–805) cm^{-1} is confirmed and supported by (Yu-Fang Lee et al., 2015).

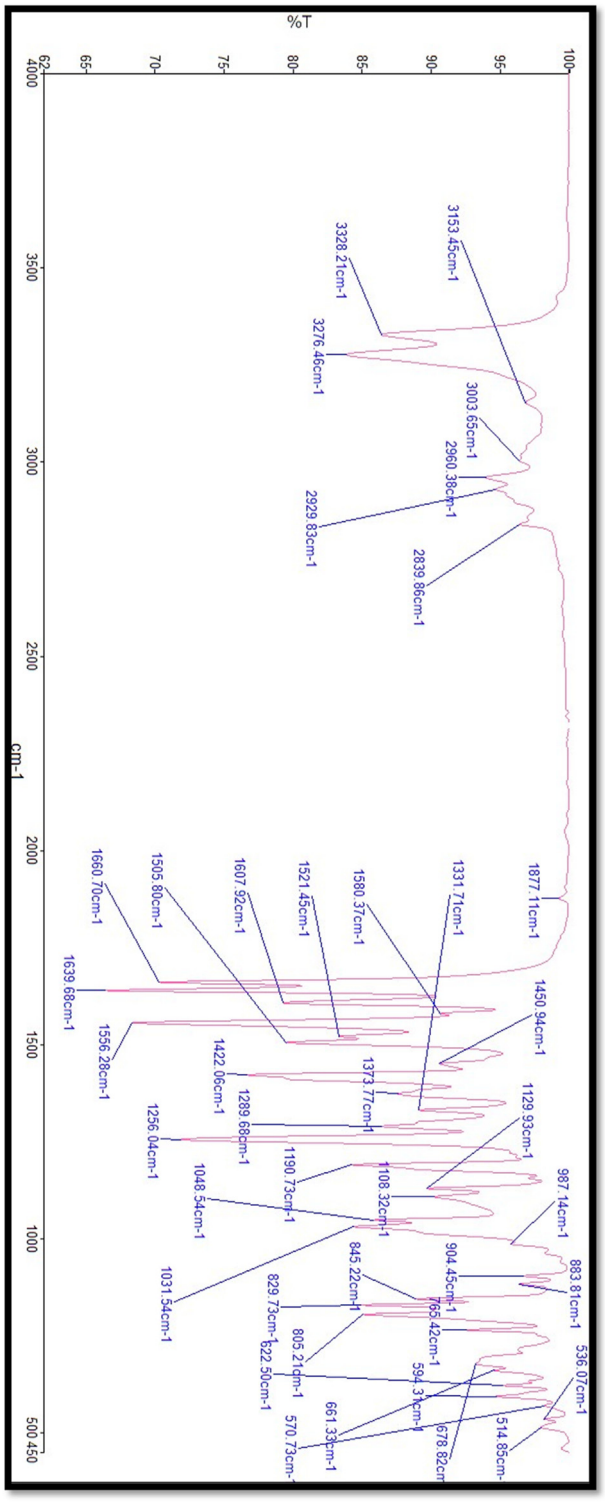

Fig. 4. FTIR spectrum of agent L1.

The TGA was in the 10 to 800 °C range, the nitrogen flow and heating rate were 50 ml/min (Fig. 5). TGA data are summarized in (Table 3) and proved that there is a matching in the losing weight between the suggested and calculated formulae. Agent L1 displayed a steady part till 360 °C. The first stage occurs in the range 360–550 °C with a loss in weight equal to 89.38% (89.47%) referring to the $C_{23}H_{22}N_2O_3$ molecule. The complete dissociation of agent L1 occurs in the 600–800 °C range leaving the CH_3 molecule.

Previous studies showed by the western blot technique, that HSP27 is highly expressed in ovarian cancer cell lines such as (SKOV3, OVCAR3, and HEY1B) (Kuo et al., 2015; Jaragh-Alhadad, 2018; Alhadad et al., 2020). In addition, HSP27 is highly expressed in both SKOV3 and SKBR3 cell lines (Jaragh-Alhadad et al., 2022). Moreover, Lama et al., proved that HSP27 is overexpressed in both monolayer and spheroids of H292 cells (Lama et al., 2015). Based on that, agent L1 was designed and synthesized to target HSP27 protein in the lung (H292), ovarian (SKOV3), and breast (SKBR3) cancer cell lines in-vitro. The data summarized in (Table 4) showed that agent L1 is cytotoxic and demonstrated potent anti-cancer activity at the micro-molar concentration. Cancer cells were treated with 25 μM of agent L1 and the data revealed that cancer cell death was pronounced first in breast cancer cell line (SKBR3) with IC_{50} value ranges 1.57 μM, followed by ovarian cancer (SKOV3) ranges 2.63 μM and then in lung cancer (H292) ranges 8.87 μM. HEK293 cells; were used as our healthy cells.

In 2006, in a clinical trial of 773 patients treated with bevacizumab in combination with paclitaxel-carboplatin treatment for lung cancer, the result showed an improved response rate reached ($P < 0.001$) (Sandler et al., 2006). Shen et al. investigated SKOV3 cell proliferation following OCT 20 μg/ml treatment, significantly reduced the IC_{50} value ($P < 0.05$), and promoted apoptosis ($P < 0.05$) in response to cisplatin. (Shen et al., 2011). Jian et al. used hyaluronic acid-nimesulide conjugate targeting HT-29 cells and the results showed nimesulide cell killing ability at 400 μM (Jian et al., 2017). Furthermore, in the study hypopharyngeal carcinoma cells were exposed to nimesulide with different concentrations ranging 10–1000 μM, a time-dependent experiment showed cytotoxicity reach ($P < 0.05$). In sum, the NSAIDs' derivative agent L1 IC_{50} values were significantly potent compared to those attained in previous studies and trials. Therefore, this confirms agent L1 as an anticancer agent.

4. Discussion

Most of the NSAIDs inhibit cyclooxygenase enzyme COX-2 prostaglandins inflammatory mediator (Bennett and Villa, 2000; Sobolewski, et al., 2010), which cause the anti-inflammation and antipyretic activities (Famaey, 1997; Hawkey, 2001). However, the mechanism of action of NSAID, safety, and efficacy are still limited. The development of safe and effective chemotherapeutic drugs is needed (Thun et al., 2002) because NSAIDs increase liver toxicity (Bessone, 2010). NSAIDs such as bromfenac, ibufenac, and benoxaprofen, have been withdrawn from the market due to hepatotoxicity; others like nimesulide were never marketed in some countries such as the USA and withdrawn in others (Bessone, 2010), even if the incidence is fairly uniform ranging from 1 to 9 cases per 100 000 persons exposed (Rodríguez, 1992; Rostom et al., 2005).

Therefore, the discovery of new COX-2 nimesulide inhibitors with low cytotoxicity is the biggest challenge in pharmaceutical research these days. A research study stated that NSAIDs, including indomethacin, piroxicam, sulindac, and aspirin, have a potent inhi-

Table 3
The analytical and physical data of agent L1.

Agent	M.W., m/e Calcd. (Found)	Color	M.P., ° C	C% Calcd. (Found)	H% Calcd. (Found)	N% Calcd. (Found)	O% Calcd. (Found)
N-(4-acetamido-3-((2,5-dimethylbenzyl)oxy)phenyl)-4-methoxybenzamide (L1)	418.48 (418.36)	White	<350	71.75 (71.63)	6.26 (6.21)	6.69 (6.73)	15.29 (15.32)
	1H NMR	NH NH 10.05 (s, 1H) 9.05 (s, 1H)	Ar-H 7.95–7.04 (m,10*H*)	CH_2 5.07 (s,2H)	OCH_3 3.83 (s,3H)	CH_3 2.50–2.04 (m,9H)	13C signals 168.21 (C=O) 149.84 (C-O) 136.48 (C-N) 105.51 (C=C) 68.49 (CH_3)
	FTIR spectra	ν(NH) 3328 (br) 3276 (br)	ν(C = O) 1660 (s) 1639 (s)	ν(C-N) 1607 (m)	ν(C-O) 1256 (s)	ν(CH_3O) (1048–1031) (829–805)	
	TGA	Middle Temp. °C 550 800		Removed species - $C_{23}H_{22}N_2O_3$ - CH_3O		Weight loss % Found (Calcd) 89.38 (89.47) 7.46 (7.41)	

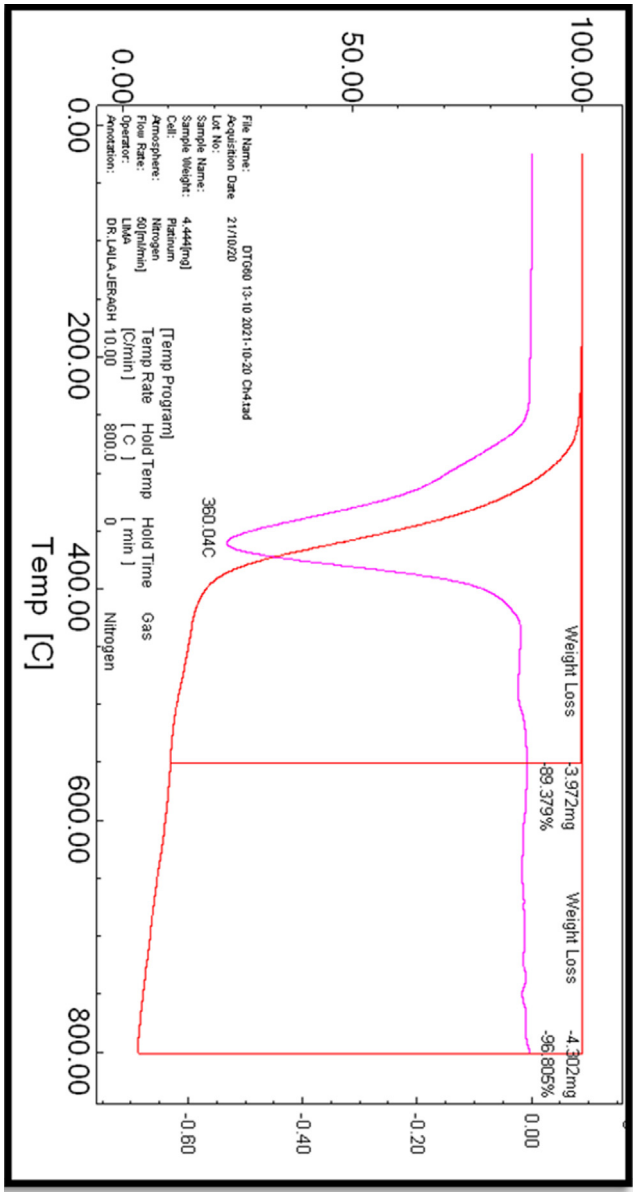

Fig. 5. The TGA thermogram of agent L1.

Table 4
Biological assessment of agent L1, after 48hr treatment.

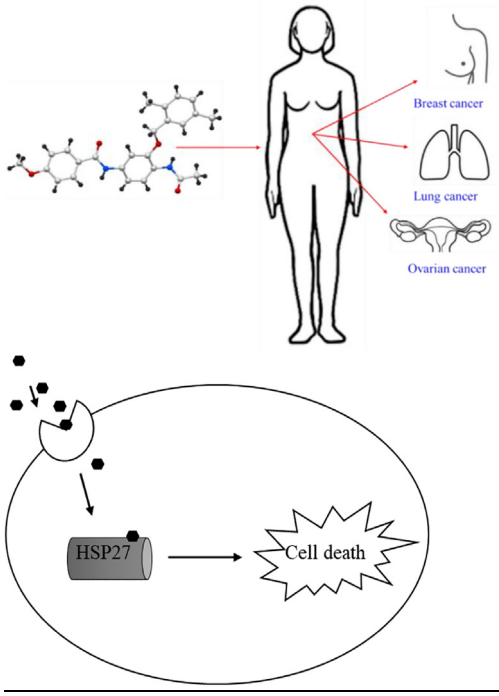

	Cell line/Group	Agent L1 treatment
IC_{50}: half inhibition concentration/ 25 μM	H292 lung cancer	8.87 ± 2.06 [a]
	SKOV3 ovarian cancer	2.63 ± 1.84[b]
	SKBR3 breast cancer	1.57 ± 0.63[c]
	HEK293 healthy kidney cells	7.02 ± 1.45 *

The experiments were done in quadruplicated and repeated at least three times, data were represented as Mean ± SD, ($P < 0.05$).
[a] Slightly above-controlled cells- HEK293 group.
[b] Significantly decreased from the controlled cells-HEK293 group.
[c] Significantly decreased from the controlled cells-HEK293 group.

bitory effect on the growth of colorectal cancer when inhibiting COX-2 activity (Hai-Ming et al., 2007). Numerous studies proved that nimesulide is a non-steroidal anti-inflammatory drug (NSAID) and is characterized for its antipyretic activities (Ward et al., 1988; Bennett and Villa, 2000; Jian-Ying et al., 2003; Catarro et al., 2019;

Güngör et al., 2021; Jaragh-Alhadad et al., 2022). Kankanala et al. synthesized and evaluated nimesulide-based novel glycol amide esters against HCT-15, human colon cancer cell line, and the agents showed anti-cancer activity (Kankanala et. al, 2013). Kim et al., used nimesulide combined radiation for the treatment of A549 lung cancer cells and the results showed increased apoptosis, induced the cleavage of caspase-3, caspase-9, and poly (ADP-ribose) polymerase (PARP), activated caspase-8, and induced cleavage of Bid (Kim et al., 2009). In addition, Alhadad et al. indirectly targeted cellular HSP27 protein and human epidermal growth factor (HER2) receptor through HER2 pathway using low-density lipoprotein (LDL) encapsulated cholesterol conjugated nimesulide derivative. The results showed LDL internalization in ovarian cancer cells and increased cell death (Alhadad et al., 2020). Furthermore, Totzke et al. used COX-2 inhibitor nimesulide to target TNF death receptor in Hela cell H21, and the data suggest that COX-2 inhibitor overcome apoptosis resistance to the extrinsic receptor-induced apoptotic pathway independently of COX-2 (Totzke et al., 2003). Also, Chu et al., stated that nimesulide could induce apoptosis and inhibit the growth of PANC–1 cells by enhancing the expression of phosphatase tensin homolog (PTEN), which indicates the potential of nimesulide to prevent tumor angiogenesis (Chu et al., 2010). On the other hand, Prevot et al., conducted a study based on the role of the prostaglandins to define the renal effects of nimesulide in 28 newborn rabbits. The data reporting neonatal acute renal failure or irreversible end-stage renal failure after maternal ingestion of nimesulide (Prevot et al., 2004).

In the present study, nimesulide derivative agent L1 was successfully synthesized and physically characterized by color, melting point, and TGA. In addition to the chemical characterization, including FTIR, 1H NMR, and 13C NMR spectra. Agent L1 was white solid, and its structure was confirmed by a single crystal with a P-1 space group. Our results confirmed that nimesulide derivative agent L1 targeted HSP27 in cancer cell lines and proved its anti-cancer activity.

5. Conclusion

Cancer is a fundamental cause of death worldwide. Therefore, old drug development is required. Nimesulide is an antiproliferation drug and produces pronounced cancer cells reduction. In conclusion, agent L1 was successfully prepared, and its structure was confirmed, spectroscopically characterized, and possessed potent anti-cancer activity with lung (H292), ovarian (SKOV3), and breast (SKBR3) cancer cell lines in the micromolar level. The overall results highlight nimesulide as an anti-cancer agent. In the future, new nimesulide derivatives will be synthesized for better biological selectivity and anti-cancer activity in both in-vitro and in-vivo models.

Declaration of Competing Interest

The authors declare that they have no known competing financial interests or personal relationships that could have appeared to influence the work reported in this paper.

Acknowledgments

This research was supported financially by Kuwait University-Research Sector under grant number SC14/18. Authors also acknowledge the RSPU at Kuwait University projects: GS01/03, GS01/05, GS02/01, and GS03/08. Also, the authors would like to thank our research team in King Saud University- Saudi Arabia represented by Dr. Fars Alanazi and Dr. Gamaleldin Harisa for their support to the success of the first series of nimesulide analogs targeting proliferation proteins in ovarian cancer.

Appendix A. Supplementary material

The crystal structure of nimesulide derivative agent L1 is deposited at Cambridge Crystallographic Data Centre (CCDC) under number 2116516. Supplementary data to this article can be found online at https://doi.org/10.1016/j.jsps.2022.03.004.

References

Aggarwal, B.B., Shishodia, S., Sandur, S.K., Pandey, M.K., Sethi, G., 2006. Inflammation and cancer: how hot is the link? Biochem. Pharmacol. 72, 1605–1621.
Aletti, G.D., Gallenberg, M.M., Cliby, W.A., Jatoi, A., Hartmann, L.C., 2007. Current management strategies for ovarian cancer. Mayo Clin. Proc. 82, 751–770.
Alhadad, L.J., Harisa, G.I., Alanazi, F.K., 2020. Design and encapsulation of anticancer dual HSP27 and HER2 inhibitor into low density lipoprotein to target ovarian cancer cells. Saudi Pharm. J. 28 (2020), 387–396.
Banti, C.N., Papatriantafyllopoulou, C., Manoli, M., Tasiopoulos, J., Hadjikakou, S.K., 2016. Nimesulide Silver Metallodrugs, Containing the Mitochondriotropic, Triaryl Derivatives of Pnictogen; Anticancer Activity against Human Breast Cancer Cells. Inorg. Chem. 55 (17), 8681–8696.
Baowei, S., Congcong, Q., Bing, L., Yong, L., Tian, F., Qingdi, Z., 2017. Increased HSP27 correlates with malignant biological behavior of non-small cell lung cancer and predicts patient survival. Sci. Rep. 7, 13807.
Bennett, A., Villa, G., 2000. Nimesulide: an NSAID that preferentially inhibits COX-2 and has various unique pharmacological activities. Expert Opin. Pharmacother. 1, 277–286.
Bessone, F., 2010. Non-steroidal anti-inflammatory drugs: What is the actual risk of liver damage? World J. Gastroenterol. 16, 5651–5661.
Calderwood, S.K., Khaleque, M.A., Sawyer, D.B., Ciocca, D.R., 2006. Heat shock proteins in cancer: chaperones of tumorigenesis. Trends Biochem. Sci. 31, 164–172.
Casado, P., Zuazua-Villar, P., delValle, E., Martínez-Campa, C., Lazo, P.S., Ramos, S., 2007. Vincristine regulates the phosphorylation of the antiapoptotic protein HSP27 in breast cancer cells. Cancer Lett. 247 (2), 273–282.
Catarro, M., Serrano, J.L., Ramos, S.S., Silvestre, S., Almeida, P., 2019. Nimesulide analogues: From anti-inflammatory to antitumor agents. Bioorg. Chem. 88.
Charette, S.J., Landry, J., 2000. The interaction of HSP27 with Daxx identifies a potential regulatory role of HSP27 in Fas-induced apoptosis. Ann. N. Y. Acad. Sci. 926, 126–131.
Chu, M., Wang, T., Sun, A., Chen, Y., 2018. Nimesulide inhibits proliferation and induces apoptosis of pancreatic cancer cells by enhancing expression of PTEN. Experimental Therapeutic Med. 16, 370–376.
Ciocca, D.R., Calderwood, S.K., 2005. Heat shock proteins in cancer: diagnostic, prognostic, predictive, and treatment implications. Cell Stress Chaperones. 10, 86–103.
Famaey, J.P., 1997. In vitro and in vivo pharmacological evidence of selective cyclooxygenase-2 inhibition by nimesulide: an overview. Inflamm. Res. 46, 437–446.
Ferreira, R.G., Narvaez, L.E.M., Espindola, K.M.M., Rosario, A.C.R.S., Lima, W.G.N., Monteiro, M.C., 2021. Can Nimesulide Nanoparticles Be a Therapeutic Strategy for the Inhibition of the KRAS/PTEN Signaling Pathway in Pancreatic Cancer? Front. Oncol. 11.
Giuliano, F., Warner, T.D., 1999. Ex vivo assay to determine the cyclooxygenase selectivity of non-steroidal anti-inflammatory drugs. Br. J. Pharmacol. 126, 1824–2830.
Güngör, T., Ozleyen, A., Yılmaz, Y., Siyah, P., Ay, M., Durdağı, S., Tumer, T., 2021. New nimesulide derivatives with amide/sulfonamide moieties: Selective COX-2 inhibition and antitumor effects. Eur. J. Med. Chem. 5 (221).
Hai-Ming, F., Qiao, M., Jian-Ming, X., Wei-Juan, M., 2007. 5-aminosalicylic acid in combination with nimesulide inhibits proliferation of colon carcinoma cells in vitro. World J. Gastroenterol. 13, 2872–2877.
Han-Shui, H., Jiun-Han, L., Wen-Chien, H., Tien-Wei, H., Kelly, S., Shih-Hwa, C., Yo-Ting, T., Shih-Chieh, H., 2011. Chemoresistance of lung cancer stemlike cells depends on activation of Hsp27. Cancer 117, 1516–1528.
Haiping, J., Hui, J., Lin, Z., Haijun, L., Kan, J., 2017. MicroRNA-577 suppresses tumor growth and enhances chemosensitivity in colorectal cancer. J. Biochem. Biomed. Toxicol. 31 (6).
Hawkey, C.J., 2001. COX-1 and COX-2 inhibitors. Best Pract. Res. Clin. Gastroenterol. 15, 801–820.
Hua, G., Xueyan, H., Lingfei, G., Xianzhi, Y., 2017. Clinicopathological significance of HSP27 in gastric cancer: a meta-analysis. Onco Targets Ther. 10, 4543–4551.
Janne, P.A., Mayer, R.J., 2000. Chemoprevention of colorectal cancer. N. Engl. J. Med. 342, 1960–1968.
Jaragh-Alhadad, L., 2018. In-vitro evaluation of HSP27 inhibitors function through HER2 pathway for ovarian cancer therapy. Transl. Cancer Res. 7, 1510–1517.

Jaragh-Alhadad, L., Harisa, G.A., Alanazi, F.K., 2022. Development of nimesulide analogs as a dual inhibitor targeting tubulin and HSP27 for treatment of female cancers. J. Mol. Struct. 1248.
Jaragh-Alhadad, L., Ali, M., 2021. Nimesulide derivatives induce apoptosis against breast and ovarian cancer: synthesis, characterization, biological assessment, and crystal structure. Kuwait J. Sci., 1–25
Jemal, A., Siegel, R., Xu, J., Ward, E., 2010. Cancer statistics, 2010. CA Cancer J. Clin. 60, 277–300.
Jian-Ying, L., Xiao-Zhong, W., Feng-Lin, C., Jie-Ping, Y., He-Sheng, L., 2003. Nimesulide inhibits proliferation via induction of apoptosis and cell cycle arrest in human gastric adenocarcinoma cell line. World J. Gastroenterol. 15 (9), 915–920.
Jian, Y.S., Chen, W.C., Lin, C.A., Yu, H.P., Lin, H.Y., Liao, M.Y., Wu, S.H., Lin, Y.F., Lai, P. S., 2017. Hyaluronic acid–nimesulide conjugates as anticancer drugs against CD44-overexpressing HT-29 colorectal cancer in vitro and in vivo. Int. J. Nanomed. 12, 2315–2333.
Jin, X., Mu, P., 2015. Targeting Breast Cancer Metastasis. Breast Cancer: Basic and Clinical Research. 9, 23–34.
Jörg, C.H., Sainitin, D., Haupt, J.V., Petra, L., Yixin, Z., Schroeder, M., 2016. New HSP27 inhibitors efficiently suppress drug resistance development in cancer cells. Oncotarget. 7 (42), 68156–68169.
Kankanala, K., Vangala, V.R., Devi, Y.P., Mangamoori, L.N., Mukkanti, K., Pal, S., 2013. Nimesulide Based Novel Glycolamide Esters: Their Design, Synthesis, and Pharmacological Evaluation. J. Chem. 816769.
Kim, B.M., Won, J., Maeng, K.A., Han, Y.S., Yun, Y.S., Hong, S.H., 2009. Nimesulide, a selective COX-2 inhibitor, acts synergistically with ionizing radiation against A549 human lung cancer cells through the activation of caspase-8 and caspase-3. Int. J. Oncol. 34, 1467–1473.
Kuo, C.L., Kyun, H., Nitin, A., Min, K.K., Kyung-Hee, K., Byong, C.Y., Hwa-Seung, Y., 2015. Reduced expression of HSP27 following HAD-B treatment is associated with Her2 downregulation in NIH: OVCAR-3 human ovarian cancer cells. Mol. Med. Rep., 3787–3794
Lama, R., Liu, D., Zhong, B., Danielpour, D., Zhou, A., Su, B., 2015. J. Cancer Res. Therap. 3, 44–51.
Mahase, E., 2019. Cancer overtakes CVD to become a leading cause of death in high income countries. BMJ 366.
Piazza, G.A., Keeton, A.B., Tinsley, H.N., Whitt, J.D., Gary, B.D., Mathew, B., Singh, R., Grizzle, W.E., Reynolds, R.C., 2010. NSAIDs: Old Drugs Reveal New Anticancer Targets. Pharmaceuticals 3, 1652–1667.
Prévot, A., Mosig, D., Martini, S., Guignard, J.P., 2004. Nimesulide, a Cyclooxygenase-2 Preferential Inhibitor, Impairs Renal Function in the Newborn Rabbit. Pediatr. Res. 55, 254–260.
Rocchi, P., Beraldi, E., Ettinger, S., Fazli, L., Vessella, L., Nelson, C., Gleave, M., 2005. Increased Hsp27 after Androgen Ablation Facilitates Androgen-Independent Progression in Prostate Cancer via Signal Transducers and Activators of Transcription 3–Mediated Suppression of Apoptosis. Cancer Res. 65 (23), 11083–11093.
Rodríguez, L.A.G., Pérez, S., Walker, A.M., Lueck, L., 1992. The role of non-steroidal anti-inflammatory drugs in acute liver injury. BMJ 305, 865–868.
Rostom, A., Goldkind, L., Laine, L., 2005. Nonsteroidal anti-inflammatory drugs and hepatic toxicity: a systematic review of randomized controlled trials in arthritis patients. Clin. Gastroenterol. Hepatol. 3, 489–498.
Sandler, A., Gray, R., Perry, M.C., Brahmer, J., Schiller, J.H., Dowlati, A., Lilenbaum, R., Johnson, D.H., 2006. Paclitaxel-Carboplatin Alone or with Bevacizumab for Non–Small-Cell Lung Cancer. N. Engl. J. Med. 355, 2542–2550.
Shen, Y., Ren, M., Shi, Y., Zhang, Y., Cai, Y., 2011. Octreotide enhances the sensitivity of the SKOV3/DDP ovarian cancer cell line to cisplatin chemotherapy in vitro. Experimental Therapeutic Med. 2, 1171–1176.
Sobolewski, C., Cerella, C., Dicato, M., Ghibelli, L., Diederich, M., 2010. The Role of Cyclooxygenase-2 in Cell Proliferation and Cell Death in Human Malignancies. Cell Stress Cell Death 2010, 1–21.
Taketo, M., 1998. Cyclooxygenase-2 inhibitors in tumorigenesis (part I). J. Natl. Cancer Inst. 90, 1529–1536.
Taketo, M. Cyclooxygenase-2 inhibitors in tumorigenesis (part II). J Natl Cancer Inst. 90, 1609-20.
Thun, M.J., Henley, S.J., Patrono, C., 2002. Nonsteroidal Anti-inflammatory Drugs as Anticancer Agents: Mechanistic, Pharmacologic, and Clinical Issues. J. Natl Cancer Inst. 94, 252–266.
Torre, L.A., Bray, F., Siegel, R.L., Ferlay, J., Lortet-Tieulent, J., Jemal, A., 2012. Global cancer statistics. CA Cancer J. Clin. 2015, 87–108.
Totzke, G., Schulze-Osthoff, K., Jänicke, R., 2003. Cyclooxygenase-2 (COX-2) inhibitors sensitize tumor cells specifically to death receptor-induced apoptosis independently of COX-2 inhibition. Oncogene 22, 8021–8030.
Vidyasagar, A., Wilson, N.A., Djamali, A., 2012. Heat shock protein 27 (HSP27): biomarker of disease and therapeutic target. Fibrogenesis Tissue Repair 5, 7.
Ward, A., Broagden, R.A., 1988. Nimesulide. A preliminary review of its pharmacological properties and therapeutic efficacy in inflammation and pain states. Drugs 36, 732–753.
Xi, C., Xiu-Shuai, D., Hai-Yan, G., Yong-Fang, J., Ying-Lan, J., Yu-Ying, C., Li-Yan, C., Jing-Hua, W., 2015. Suppression of HSP27 increases the anti-tumor effects of quercetin in human leukemia U937 cells. Mol. Med. Rep. 13, 689–696.
Yu-Fang, L., Wei-Te, C., Britta, A.J., Daniel, P.T., Edwin, L.S., Yuan-Pern, L., 2015. Infrared absorption of CH_3O and CD_3O radicals isolated in solid para-H_2. J. Mol. Spectrosc. 310, 57–67.
Zakaria, N., Abdul Satar, N., Abu Halim, N.H., Ngalim, S.H., Usoff, N.M., Lin, J., Yahaya, B.H., 2017. Targeting Lung Cancer Stem Cells: Research and Clinical Impacts. Front. Oncol. 7, 1–10.
Zaorsky, N.G., Churilla, T.M., Egleston, B.L., Fisher, S.G., Ridge, J.A., Horwitz, E.M., Meyer, J.E., 2017. Causes of death among cancer patients. Ann. Oncol. 28, 400–407.
Zappavigna, S., Cossu, A.M., Grimaldi, A., Bocchetti, M., Ferraro, G.A., Nicoletti, G.F., Filosa, R., Caraglia, M., 2020. Anti-Inflammatory Drugs as Anticancer Agents. Int. J. Mol. Sci. 21, 2605.
Zhang, D., Wong, L.L., Koay, E.S., 2007. Phosphorylation of Ser78 of Hsp27 correlated with HER-2/neu status and lymph node positivity in breast cancer. Mol. Cancer. 7 (52), 52.
Zhang, Z., Zhou, L., Xie, N., Nice, E.C., Zhang, T., Cui, Y., Huang, C., 2020. Overcoming cancer therapeutic bottleneck by drug repurposing. Signal Transduction Targeted Therap. 5, 1–25.
Zhengyong, L., Yi, L., Yupeng, L., Baohua, L., Xiangfeng, W., 2021. Role of HSP27 in the multidrug sensitivity and resistance of colon cancer cells. Oncol. Lett. 19, 2021–2027.